

# Fluke 8588A DMM Sampling Performance

Rado Lapuh, Jan Kučera, Jakub Kováč, Boštjan Voljč

**Abstract**—This paper reports on an evaluation of the Fluke 8588A digital multimeter (DMM) sampling performance and comparison to Keysight 3458A DMM sampling performance. The design of 8588A type DMM shows both similarities and striking differences in design compared to 3458A type DMM. Apart from their specified sampling capabilities, measurements were performed to evaluate frequency response, noise performance, including a  $1/f$  type noise and a timing jitter induced noise, as well as phase measurement performance.

**Index Terms**—Measurement, sampling, amplitude response, phase response, harmonics, measurement uncertainty, Josephson voltage source.

## I. INTRODUCTION

SOON after the 3458A DMM was introduced to a market in 1988, metrologists in the National Metrology Institutes (NMI) started using its novel sampling capabilities for various measurements, achieving groundbreaking performance increase, particularly in terms of lowering measurement uncertainties [1, 2, 3, 4, 5, 6, 7] in various measurement areas. This was achieved by using a custom made multi-slope integrating analogue-to-digital converter (IADC), which exhibits a few key properties built in by design. First, the IADC has a variable resolution, which is a function of a programmable aperture time. Second, the aperture time provides for a calculable filter, which effectively attenuates high frequency (interference) signals before they can interfere with the resulting quantisation process. Third, this filter function can be equalised almost exactly even for a large attenuation values, achieving a correction ratios of up to 5000:1 [1]. This resulted in a state of the art sampler for low frequency signals [8].

The IADC technique has since evolved into a wildly popular delta-sigma conversion technique [9]. The NI-5922 flexible resolution digitiser became popular in many NMIs for performing state of the art measurements and it arguably offers the top performance that delta-sigma conversion technique can deliver. However, its performance never challenged the 3458A performance at low frequency sampling applications. After three decades, the Fluke 8588A multimeter (DMM) appears to be the first DMM in almost thirty years to challenge the state of the art Keysight 3458A DMM sampling performance. The first evaluation of its sampling performance with comparison to 3458A is presented in this paper. The discussion is limited solely for sampling voltage signals. As this evaluation only deals with sampling voltage signals, it can in no case prejudice complete performance of any instrument discussed.

R. Lapuh is with the Metrology Institute of the Republic of Slovenia, 3000 Celje, Slovenia, (e-mail: rado.lapuh@gov.si). Jan Kučera and Jakub Kováč are with Czech Metrology Institute (CMI), Okružní 31, 638 00 Brno, Czech Republic. B. Voljč is with Slovenian Institute of Quality and Metrology,

A precision ČMI SWG03 DDS source [10] and Keysight 33622A arbitrary waveform synthesizer [11] were used for all measurements requiring a sine wave input signal.

## II. ADC TECHNOLOGY

### A. DMM ADC

DMMs are primarily intended to accurately measure voltage, current, resistance and possibly other quantities. To achieve this, the ADC used must be stable, linear and have a high resolving resolution, while the high conversion speed is not required. The ADC technology of choice is an integrating or charge balance ADC (IADC), dominating the DMM market for decades. Its multi-slope version, developed for then Hewlett-Packard 3458A provided for an unprecedented performance increase in stability, linearity and resolution. Importantly, this was not sacrificed by an excessively slow performance. On the contrary, also the maximum sampling rate was increased from a solid 1350 Hz in previous model (HP 3457A) [12] to a then whooping 100 kHz for an IADC while still maintaining 16 bit resolution [13]. To cope with even higher frequency repetitive signals, the sample-hold circuitry is employed to freeze a signal until it is converted by its IADC. This circuitry allows for only 50 kHz sampling frequency, but a short aperture time of 2 ns allows for a sub-sampling scheme, technically employing 100 MHz sampling rate and capturing repetitive signals with frequencies approaching 50 MHz. However, this sample-hold measurement path is far less accurate than a direct DCV path.

8588A type DMM introduces a slightly different concept, using IADC (Fluke calls this type of ADC a Charge Balancing ADC or CB) for slow sampling rates up to 4.7619 kHz and an 18 bit successive approximation (SAR) ADC for fast sampling rates up to 5 MHz. Additionally, as a new product, 8588A offers much larger internal memory (15 M samples) and a set of interfaces for transferring commands and data (GPIB, USB and Ethernet). The CB and SAR technologies are said to work together[14] for the best precision and best digitisation, but it is not disclosed neither how this is implemented nor what are the actual benefits, except of actually covering combined sampling rates from 0.1 Hz up to 5 MHz. 8588A actually provides for three modes of operation[14, 15]:

- CB mode can be used for aperture times from 100  $\mu$ s up to 10 s, with minimum trigger interval equal to aperture time plus 170  $\mu$ s. 25  $\mu$ s is used for balancing zero before the measurement aperture and 85  $\mu$ s is used afterwards for sub-reference ramps of the multi-slope operation. There seems to be an additional 60  $\mu$ s necessary for the internal processing before a new valid trigger can be accepted. The CB mode is the most stable and the most accurate mode of operation[16].

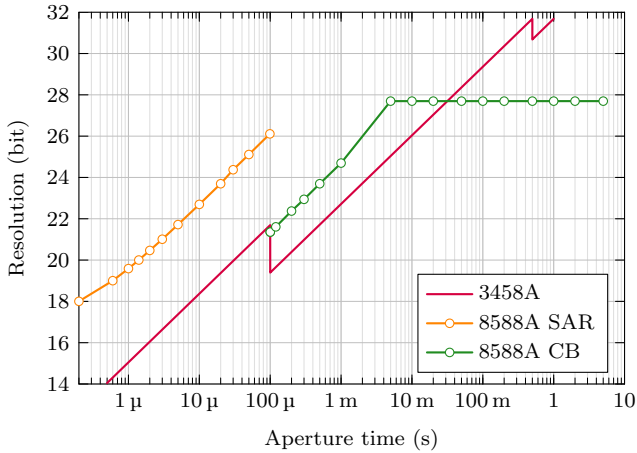


Figure 1. DMM analogue to digital converter resolving resolution in bits for nominal Range input level. Circles denote points in which this resolution was extracted from sampled data. For 3458A, this was achieved on more points, which are not indicated on this graph.

- SAR mode can be used for aperture times below  $100\ \mu\text{s}$  down to "zero" aperture time. Here the aperture is emulated by averaging the required number of samples from SAR ADC, which is internally sampling at 5 MHz sample rate. Additional  $30\ \mu\text{s}$  is required at each conversion, yielding a highest sampling frequency of 33.333 kHz. The use of this additional  $30\ \mu\text{s}$  time is not disclosed.
- DIGITIZE (DIG) mode employs the SAR DAC directly, without any additional delays, enabling the full 5 MHz sampling speed. Aperture time is still programmable from 0 ns to 3 ms and it uses the same technique as in SAR mode to emulate the analogue CB aperture time function. Manufacturer voltage accuracy specifications[16] for SAR mode and Digitizing mode are virtually the same.

### B. DMM sampling resolution

The sampling resolution discussed in this report refers to the ADC quantisation resolution and not to the usual DMM resolution specification, which also includes other imperfections like differential non-linearity and noise[17]. The sampling resolution can be easily determined by reading a scale factor which is used to convert binary values back to voltage values[18]. This was used to retrieve the 3458A sampling resolution, but was not a useful approach for 8588A as this function was not working on the available pair of 8588A. Alternatively, a number of samples were taken with input terminals shorted and the record was sorted from the lowest to the highest value measured. The minimum step was easily retrieved, indicating the ADC numerical resolution at a number of aperture times selected. The retrieved sampling resolution for both DMMs is shown on figure 1. The SAR sampling resolution increases with the increasing aperture time as the averaging function provides for the otherwise fixed SAR ADC resolution increase. Further, 8588A type DMM provides for a higher sampling resolution than 3458A type DMM from  $100\ \mu\text{s}$  to 30 ms aperture time. However, from 4 ms aperture time and longer, the 8588A limits the CB ADC resolution

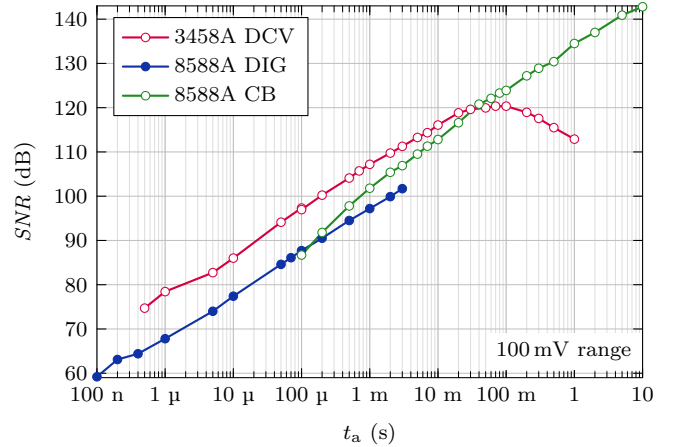


Figure 2. 100 mV range signal to noise ratio.

at 28 bits, while 3458A limit is imposed at 32 bits. Again, the sampling resolution described here is not providing any meaningful DMM performance parameter, but it provides an upper limit of internal ADC resolving power and perhaps a glimpse on its internal operation.

### III. DMM NOISE PERFORMANCE

There is a difference in the 8588A DMM design that has to be noted here to better understand the performance being reported later on. Its CB mode signal path 28 kHz bandwidth is much lower than the 3458A's DCV 150 kHz bandwidth. This would, in principle, reduce the overall noise of the DMM, with the price paid on the limited frequency response linearity at low frequencies. Further, 8588A employs chopper amp stabilisation to achieve superior offset performance [14]. This would push the pink noise corner frequency to much lower values, but could potentially degrade the overall signal to noise ratio.

#### A. Signal to Noise Ratio

The signal to noise ratio was measured by short circuiting the input terminals and performing sampling at different aperture times. 128 samples were taken in a sample burst and three bursts were taken to further average the result at each aperture time. Sampling frequencies were chosen so as to cancel the mains signal frequency interference. From the burst samples, the noise voltage  $\sigma_n$  was estimated as a median value of the FFT spectrum noise amplitude, thus rejecting interference signals originating from the mains frequency signal or other sources producing steady frequency signals. The SNR was finally calculated as a ratio of nominal range RMS voltage  $R/\sqrt{2}$  to the noise voltage

$$SNR = \frac{R}{\sigma_n \sqrt{2}}, \quad (1)$$

Results show a stark performance difference in signal to noise ratio between 3458A (DCV mode) [19] and 8588A (CB mode) DMMs. At aperture times from  $100\ \mu\text{s}$  up to 10 ms, the 3458A SNR is larger from 20 dB to 15 dB on

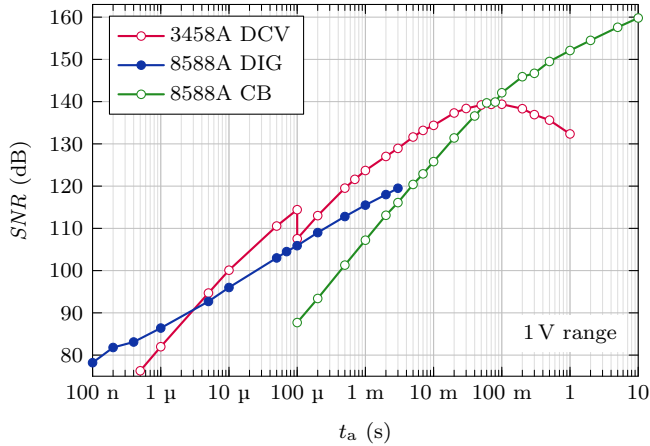


Figure 3. 1 V range signal to noise ratio.

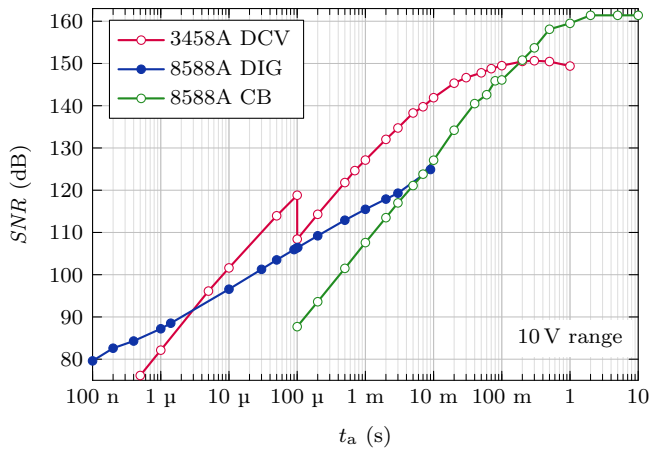


Figure 4. 10 V range signal to noise ratio.

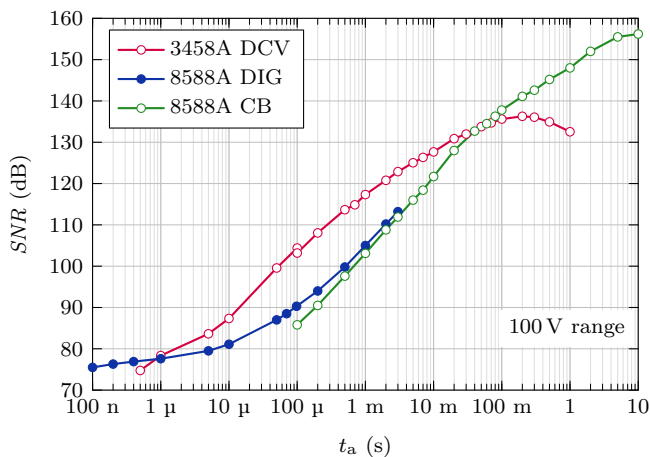


Figure 5. 100 V range signal to noise ratio.

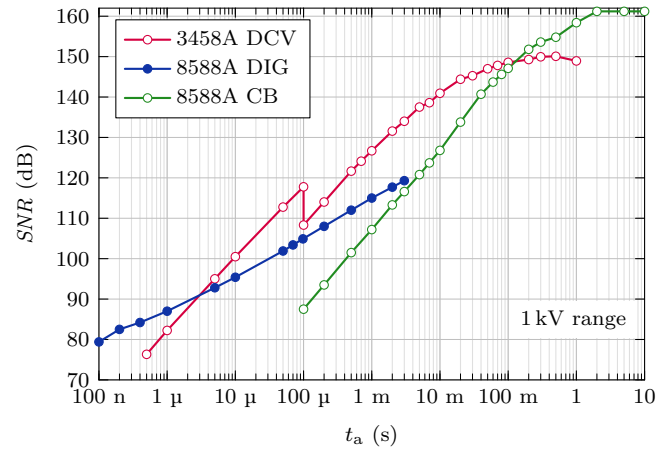


Figure 6. 1 kV range signal to noise ratio.

10 V and 1 kV ranges. This difference is smaller on other ranges where the input stage amplifiers plays a more dominant role. From aperture time at around 100 ms and up, the  $SNR$  of 3458A stops increasing and actually starts to decrease due to increasing  $1/f$  noise [18], while the  $SNR$  of 8588A increases further up to 161.4 dB, being actually limited by the 28 bit resolution limit of the CB analogue to digital converter. The 8588A DIG  $SNR$  performance, which was found to be virtually identical to its SAR performance at aperture times below 100  $\mu$ s, shows a slower increase with increasing aperture time. Nevertheless, the  $SNR$  in DIG mode is better than in CB mode for all aperture times available for DIG mode (up to 3 ms, except on 100 mV range, where the input amplifier reduces the  $SNR$  in DIG mode by 20 dB across all aperture times).

### B. $1/f$ Noise

$1/f$  noise was measured in such a way that a long continuous sampling bursts were captured in a record and an FFT was used to estimate the noise spectral density frequency response [20]. Number of samples in a record was chosen so as to effectively cover the lowest frequency of interest with a fixed sampling time of 9 ms. For 3458A, this frequency was 3 mHz and for 8588A in CB mode, this frequency was 100  $\mu$ Hz. To reach this low frequency result, the record length of up to 1 000 000 samples was required, which resulted in continuous sampling lasting up to 2.5 h for a single record. Internal timer was used to dictate the sampling time.

A single non-windowed FFT results in a fairly noisy linear spectral density. That noise can be smoothed out by averaging FFT results from more sample bursts, but in this case where a single sample burst takes minutes or even hours, this technique becomes even more time consuming. Instead, a single record was used for averaging at higher frequencies by splitting the record into more equal length sub-records, performing FFT and averaging the results. The original record was split into two, three, four and so on equal length sub-records and the lowest frequency FFT result, not influenced by a residual DC level leakage (this typically being a second or a third FFT bin) was recorded as a final result. This way, the resulting

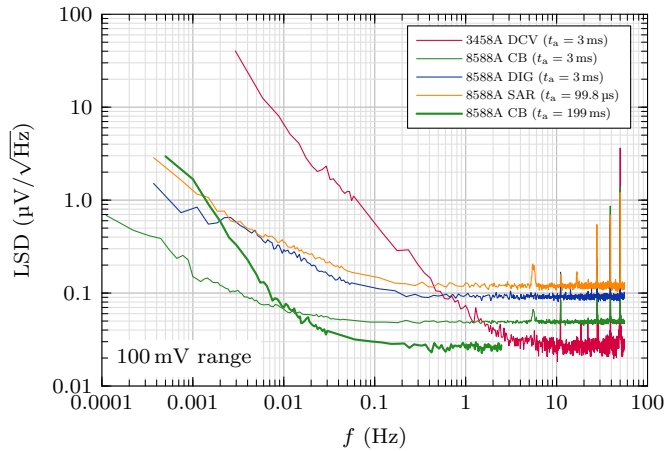


Figure 7. 100 mV range  $1/f$  noise spectral density.

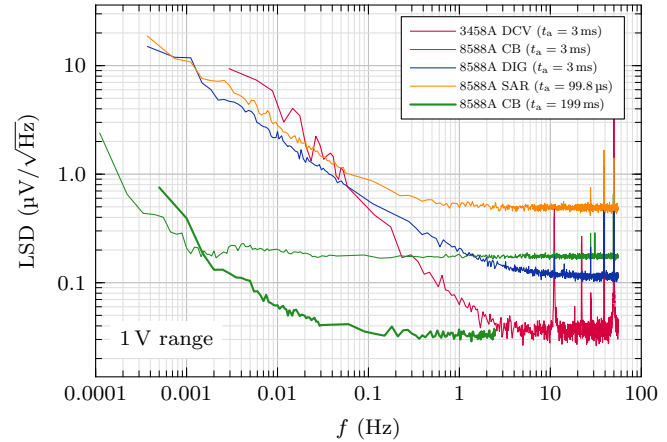


Figure 8. 1 V range  $1/f$  noise spectral density.

linear spectral density was gradually smoothed toward higher frequencies. Results are shown on Figures 7 to 11. They are collected together for each of five DMM ranges and cover five responses each:

- 3458A IADC response at 3 ms aperture time and covering frequencies from 3 mHz to 55.6 Hz.
- 8588A CB response at 3 ms aperture time and covering frequencies from 100  $\mu$ Hz to 55.6 Hz.
- 8588A CB response at 3 ms aperture time and covering frequencies from 500  $\mu$ Hz to 2.47 Hz.
- 8588A SAR response at 99.8  $\mu$ s aperture time and covering frequencies from 370  $\mu$ Hz to 55.6 Hz.
- 8588A DIG response at 3 ms aperture time and covering frequencies from 370  $\mu$ Hz to 55.6 Hz.

Frequency spikes between 10 Hz and 55.6 Hz are a byproduct of mains voltage frequency components and possibly other internal DMM or external sources and can be ignored in terms of pink noise analysis. 8588A clearly has a stronger white noise component compared to 3458A at 3 ms aperture time, supporting the measurements and discussion from the previous chapter. However, 8588A excels in  $1/f$  corner frequency, which is pushed down to 10 mHz or so on 100 mV range, and further down to 1 mHz or so on all other ranges. It appears that the 8588A SAR mode is much more noisy than 8588A DIG mode, presumably due to CB zero operation that precedes each measurement in this mode and adds its own noise to the final result. The  $1/f$  corner frequency for 8588A DIG and 8588A SAR modes seems to be one order of magnitude or so lower than  $1/f$  corner frequency for 3458A. However, here it is more important to look on the actual level of linear spectral density, as the initial white noise for any 8588A mode is already much higher and is thus masking any earlier  $1/f$  noise to appear as dominant noise component. This in effect moves the  $1/f$  corner frequency to a lower value, so the corner frequency itself is not a complete  $1/f$  noise performance indicator and should be evaluated together with the white noise level at higher frequencies.

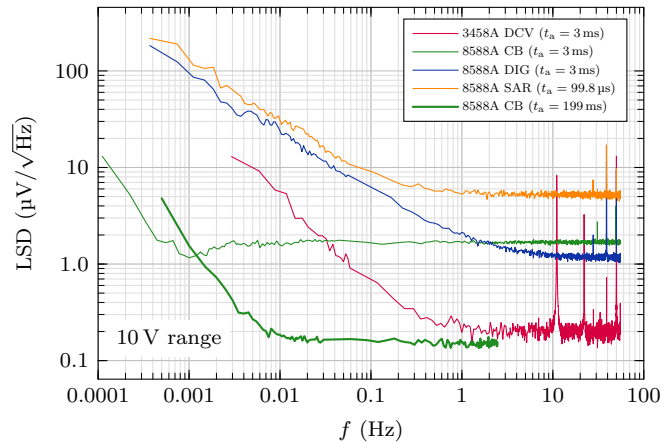


Figure 9. 10 V range  $1/f$  noise spectral density.

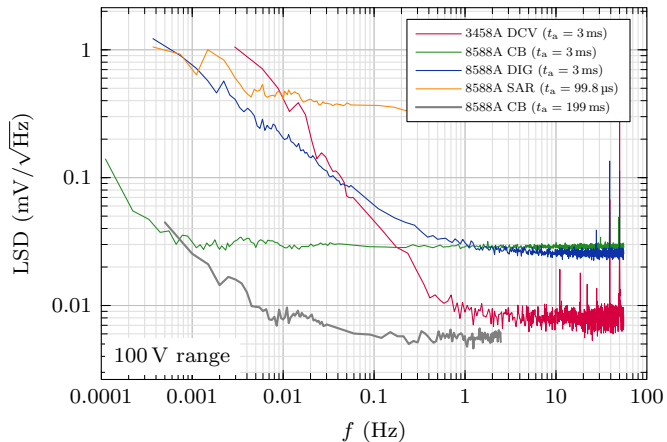


Figure 10. 100 V range  $1/f$  noise spectral density.

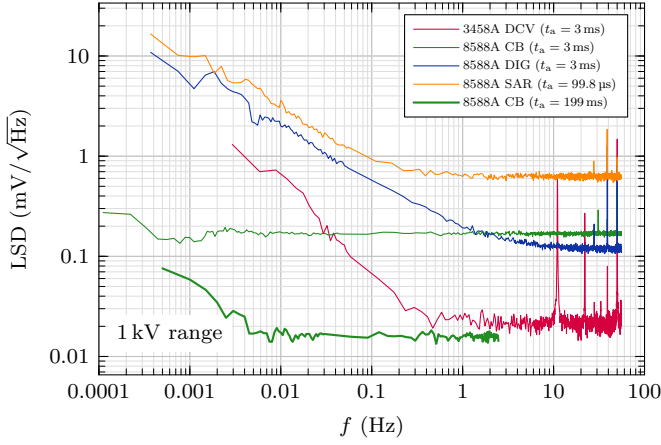


Figure 11. 1 kV range  $1/f$  noise spectral density.

### C. Jitter Noise

Jitter noise appears in a sampled signal as a consequence of sample timing variations [21]. A signal to noise ratio due to a random sampling time jitter is given by

$$SNR_j = -20 \cdot \log_{10}(2\pi ft_j), \quad (2)$$

where  $f$  is signal frequency and  $t_j$  is a standard deviation of the time jitter.  $SNR_j$  defined here is referenced to the signal amplitude applied, from where it is clear that the jitter noise is not existent if there is no signal applied. From the equation (2) it follows that for increasing signal frequency the  $SNR_j$  will drop by 20 dB per decade. The combined  $SNR_c$  is given by

$$SNR_c = -20 \cdot \log_{10} \sqrt{\left(\frac{\sigma_n}{V}\right)^2 + (2\pi ft_j)^2}, \quad (3)$$

where  $\sigma_n$  is a white noise RMS voltage.  $\sigma_n$  limits the highest achievable  $SNR_c$ , which starts to roll down as the  $SNR_j$  becomes the dominant  $SNR_c$  component.

Measurements were performed by using fixed DMM sample parameters in each mode and sampling full scale input sine wave signal at different frequencies. The shortest available aperture times were used so that aperture roll-off would not affect measurement results. It is further important that the sine wave amplitude remains flat within approximately  $\pm 0.5$  dB over the whole tested frequency range. Additionally, it is important that the source  $SNR$  at highest frequencies remains higher than the measured  $SNR$  as estimated from the sampled values. That would assure that the DMM jitter and not the source jitter is measured. A Keysight 33622A arbitrary waveform synthesizer with amplitude flatness of  $\pm 0.25$  dB for frequencies up to 60 MHz and specified time jitter of 2 ps would meet those requirements. Measurement results plotted on Fig. 12 clearly show behaviour described by (3), where the results for 3458A are taken from [21]. The time jitter values shown in Table I were deduced from this measurement results using Equation 3. For the 8588A in DIG mode result and lacking any performance test on the source, it is not completely clear if the DMM or the Keysight 33622A was the source of  $SNR$  roll off. Nevertheless, the results safely conclude that the 8588A time jitter in DIG mode is  $\leq 7.7$  ps.

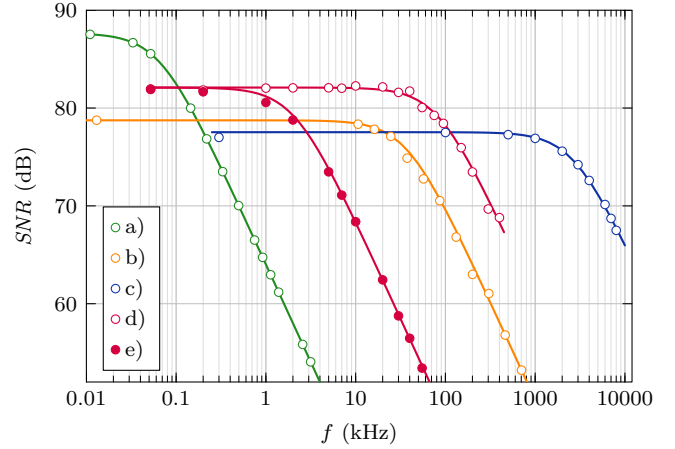


Figure 12. 8588A DMM charge balance ADC jitter noise induced signal to noise ratio roll-off. a) 8588A in CB mode (sample: TIMER), b) 8588A in SAR mode (sample: TIMER), c) 8588A in DIG mode (sample: TIMER), d) 3458A in DCV mode (sample: TIMER), e) 3458A in DCV mode (sample: EXT). 3458A in DCV mode using a Master Slave synchronisation is not plotted as it is virtually identical to e).

Table I  
ESTIMATED EFFECTIVE JITTER NOISE VALUES FROM RESULTS PLOTTED ON FIG. 12.  $t_s$  AND  $t_a$  ARE SAMPLING PARAMETERS USED FOR EACH DMM AND MODE COMBINATION MEASUREMENTS.

DMM	Mode	Timebase used	$t_s$	$t_a$	$t_j$
3458A	DCV	Timer	10 $\mu$ s	1 $\mu$ s	145 ps
3458A	DCV	External	10 $\mu$ s	1 $\mu$ s	6 ns
3458A	DCV	Master-Slave	10 $\mu$ s	1 $\mu$ s	6.8 ns
8588A	CB	Timer or External	20 $\mu$ s	110 $\mu$ s	100 ns
8588A	SAR	Timer or External	30 $\mu$ s	0 s	493 ps
8588A	DIG	Timer or External	200 ns	0 s	$\leq 7.7$ ps

## IV. DMM AMPLITUDE RESPONSE

### A. Aperture time roll-off

The integrating analogue to digital converter (or sometimes called a charge balance converter) introduces a sinc roll-off

$$H_{t_a} = \frac{\sin(\pi ft_a)}{\pi ft_a}, \quad (4)$$

with a phase offset originating directly from the time delay introduced by one half of the aperture time

$$\Phi_{t_a} = \pi ft_a, \quad (5)$$

where both (4) and (5) proved to be highly accurate[1, 18] and precisely correctable for virtually any usable product of  $ft_a$ [18, 22]. It is worth noting that IADC resolution increases with an increasing aperture time, as the IADC has more time to integrate the input voltage and hence achieve higher resolving resolution. However, the final effective resolution obtained is almost always limited by the stability and noise of the whole system, but sometimes surprisingly with the internal numerical resolution of the digital firmware involved, as seems to be a case with 8588A at aperture times above 2 s or so.

Instead of using integrated analogue to digital converter, a sample-and-hold based analogue to digital converter, for example

successive-approximation ADC with a sample-and-hold circuitry in the front-end, can be used to mimic the aperture time behaviour of the integrated analogue to digital converter by using averaging. This was employed in Fluke 8588A DMM, where SAR ADC is always used to perform analogue to digital conversion for aperture times below 100  $\mu\text{s}$  or effectively for sampling frequencies above 4.7619 kHz. This way, SAR ADC can be used in a digitising mode to cover average aperture times up to 3 ms. The SAR ADC is operating at a constant sampling frequency ( $f_{\text{sd}} = 5 \text{ MHz}$  is a fixed value for Fluke 8588A) and the resulting conversion is calculated as an average over the programmed aperture time  $t_{\text{ad}}$

$$U_{t_{\text{ad}}} = \frac{\sum_{n=1}^Q U_n}{Q}, \quad (6)$$

where  $U_n$  are individual readings from the SAR ADC conversion taken during that aperture time and  $Q$  is the number of samples used for one average value calculation. With a given sampling time  $t_{\text{sd}}$  and the number of samples taken  $Q$ , we get the resulting digital aperture time

$$t_{\text{ad}} = Qt_{\text{sd}}, \quad (7)$$

emulating the actual behaviour of the integrating (or charge balance) analogue to digital converter. This process also introduces the frequency dependent roll-off [23], similar but not equal to (4)

$$H_{t_{\text{ad}}} = \frac{\sin(\pi Q \bar{f})}{Q \sin(\pi \bar{f})}, \quad (8)$$

where  $\bar{f}$  is normalised signal frequency

$$\bar{f} = \frac{f}{f_{\text{sd}}}, \quad (9)$$

Eq. (8) can be rewritten into

$$H_{t_{\text{ad}}} = \frac{\sin(\pi f t_{\text{ad}})}{t_{\text{ad}}/t_{\text{sd}} \sin(\pi f t_{\text{sd}})}. \quad (10)$$

which more closely resembles the  $H_{t_a}$  given by (4).  $H_{t_{\text{ad}}}$  closely follows  $H_{t_a}$  for  $\bar{f} \ll 1$ , but has a smaller attenuation of any frequency component approaching or being above  $\bar{f}$  and a distinctive peak response at (no attenuation at exactly that frequencies) and around the positive integer multiples of  $\bar{f}$ . Figure 13 plots both  $H_a$  and  $H_{\text{ad}}$  for the case  $t_a = t_{\text{ad}}$  for 100 samples being used for one averaging measurement result ( $Q = 100$ ).

### B. Input filter roll-off

For frequencies up to 20 kHz, the 3458A input filter amplitude response is often modelled with a single pole RC filter[1]

$$H_{1p} = \frac{1}{\sqrt{1 + \left(\frac{f}{f_{3\text{dB}}}\right)^2}}, \quad (11)$$

since its amplitude response was already shown to closely resemble the DMM response up to a few kHz[24], despite the input circuitry actually consists of two equal serially connected RC networks with 1% tolerance 5 k $\Omega$  resistors

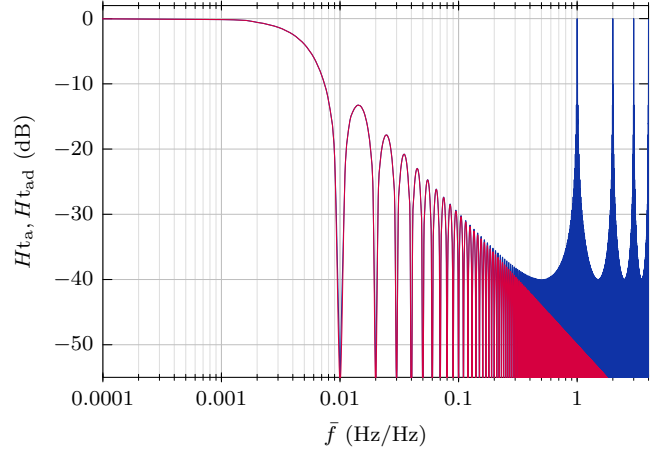


Figure 13. IADC and averaging frequency response as a function of normalised frequency, where integration time  $t_a$  for IADC (red curve) equals the averaging time  $t_{\text{ad}}$  for SAR.  $Q = 100$ ,  $t_a = t_{\text{ad}} = t_{\text{sd}}/Q$ .

Table II  
NOMINAL FREQUENCY BANDWIDTHS FOR 8588A DMM VOLTAGE SAMPLING MODES. VALUES MARKED WITH \* ARE NOT SPECIFIED BY A MANUFACTURER.

Mode	Filter	$f_{3\text{dB}}$	filter poles
CB	-	13.8 kHz*	1
SAR	-	100 kHz*	1
DIG	100 kHz	100 kHz	1
DIG	3 MHz	3 MHz	4
DIG	Off	15 MHz - 20 MHz	-

and 2% tolerance 82 pF capacitors. The single pole RC filter model would implicate phase response

$$\Phi_{1p} = \tan^{-1} \left( \frac{f}{f_{3\text{dB}}} \right). \quad (12)$$

The 8588A DMM nominal frequency response depends on the sampling mode and is collected in Table II for 10 V range. Measured frequency responses for all ranges and modes for both DMM types are plotted on Figures 14 to 18. All measurements were performed by applying a sine wave from arbitrary waveform synthesizer at selected frequencies and estimating a measured amplitude using an asynchronous PSFE sine wave amplitude estimation algorithm [25]. A 120 MHz synthesizer bandwidth secured a sine wave level constant enough for the purpose over all applied frequencies up to 20 MHz. A full range voltages were set for 100 mV, 1 V and 10 V ranges. A 7.07 V amplitude was used on 100 V and 1 kV ranges, which still provided a reasonable measurement for DMM bandwidths up to 100 kHz or so, despite significantly decreased signal to noise ratio. However, for higher bandwidths on 100 V and 1 kV ranges, the measured results plotted on figures 17 and 18 show deviation from a smooth low pass filter response. This response might be attributed to the internal 8588A DMM voltage divider.

The measured responses show almost identical frequency bandwidth between 3458A DCV mode and 8588A SAR mode. The 8588A CB mode provides a very narrow band-

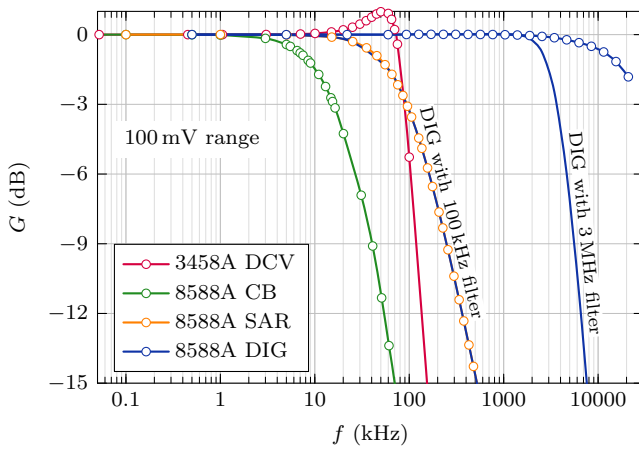


Figure 14. 100 mV range frequency response. The 8588A digitising mode with 100 kHz filter overlaps almost completely with the 8588A SAR response.

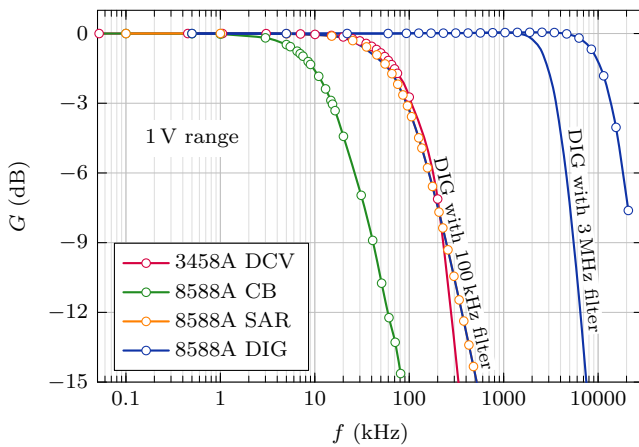


Figure 15. 1 V range frequency response.

width of 13.8 kHz, which already impacts a 50 Hz signal by  $-6.6 \mu\text{V}/\text{V}$ .

### C. Distortions

While performing tests in 8588A CB mode using a precision ČMI SWG03 [10] voltage source and observing frequency spectrum obtained, two specific results were noted. First was an elevated noise floor at signal frequencies above around 10 Hz due to the internal 8588A 100 ns time jitter (see Figure 12). Second were a persistent third and fifth harmonic components, being clearly visible at signal frequencies above 1 Hz. Figure 19 plots THD as a function of input signal frequency. As the THD of the ČMI SWG03 source was not estimated separately, two DMMs were connected to the same signal in parallel. Their measured THD is plotted as 8588A (DIG) and 3458A (DCV) and demonstrates the source THD, being equal to 3458A (DCV) plotted curve or better. Table III lists sampling parameters that were used for all three cases at each test frequency. Measurements were performed in a master-slave configuration and at each frequency two measurements were performed with the 8588A DMM in CB mode operating as a master and as a slave. Apart from reducing the SNR of

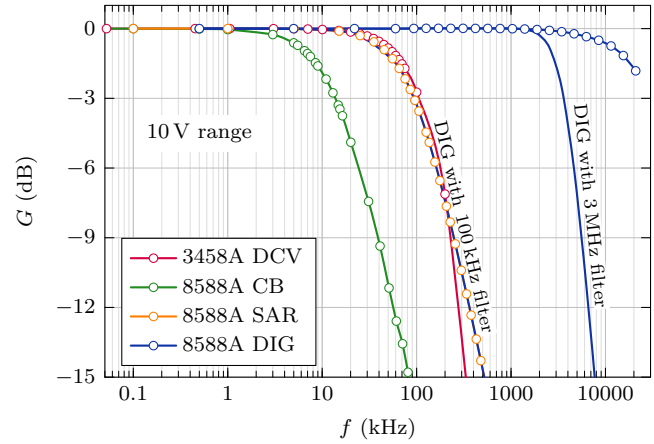


Figure 16. 10 V range frequency response.

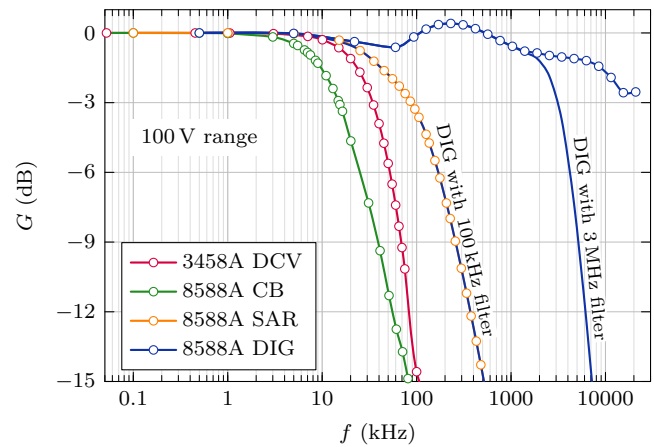


Figure 17. 100 V range frequency response.

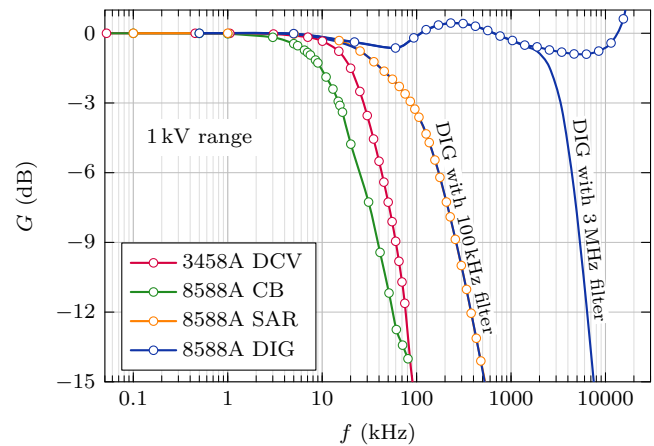


Figure 18. 1 kV range frequency response.

Table III  
DMM SAMPLING PARAMETERS USED TO PERFORM THD MEASUREMENTS. SIGNAL RMS AMPLITUDE WAS 7 V.

$f$	$t_s$	$t_a$	$N$
10 mHz	1 s	980 ms	1000
93 mHz	90 ms	89 ms	10 000
930 mHz	9 ms	1 ms	10 000
10 Hz	1 ms	890 $\mu$ s	37 888
52 Hz	1 ms	890 $\mu$ s	40 000

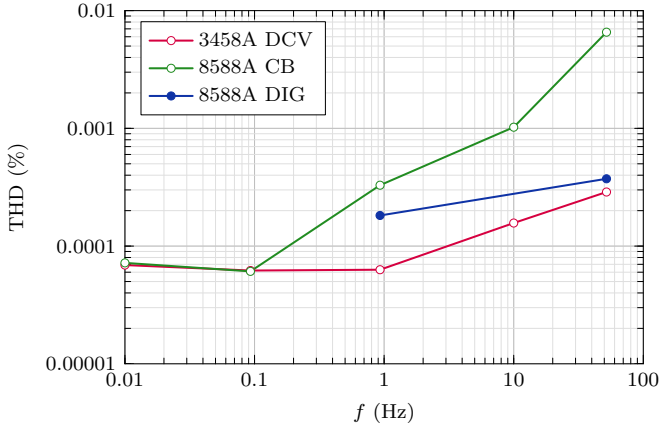


Figure 19. 8588A DMM charge balance ADC total harmonic distortions. 3458A DMM and 8588A DMM in DIG mode distortions are plotted measuring the same signal source with the same sampling parameters.

the slave DMM when 8588A DMM in CB mode was used as a master and consequently masking the harmonics of that slave SNR at frequencies above 10 Hz, THD results of the 8588A DMM in CB mode were not differing significantly between master and slave mode. A multi-frequency sine fitting algorithm [26] was used to estimate THD. The 8588A operating in CB mode shows an elevated harmonic distortions at and above 1 Hz. Figure 20 plots a spectrum of the same signal obtained by 8588A and 3458A. A multi-frequency sine

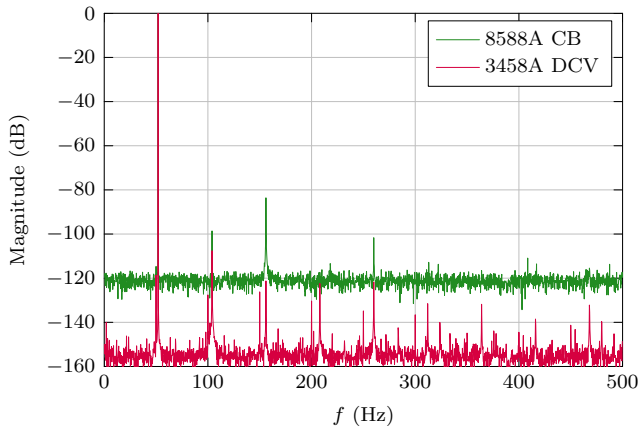


Figure 20. 8588A DMM CB mode and 3458A DCV mode spectrum while sampling 52 Hz signal with  $t_s = 1$  ms,  $t_a = 890$   $\mu$ s,  $N = 4000$  and  $M = 4$ . Signal source was ČMI SWG03 and signal amplitude was 7 V.

fitting algorithm was used to first remove signal components from the sampled data. FFT was used to retrieve the spectrum of this residual and harmonic components removed from the signal were placed directly into the spectrum results as signal peaks. Clearly, 8588A result is masked by the noise, but it also shows much stronger second, third and fifth harmonics, which are obviously not present in the signal. Resulting spectrum using 3458A clearly shows line frequency (50 Hz components up to the fifth harmonic, which is possible due to a very good  $-151$  dB noise floor achieved at the selected sampling parameters.

As it is expected for both 3458A and 8588A DMMs to be linear far below  $1$   $\mu$ V/V at DC input signal, this result shows that 8588A CB mode dynamic linearity is not following this expectation. However, 8588A DIG mode performs better and shows no signs of increased THD at any frequency. At 1 kHz, it was measured at 0.0025 % using the ČMI SWG03 source. At 110 kHz, it was measured at 0.018 % using the Keysight 33622A source. However, these results present the combined THD of both the source and the sampler and can only be used as a potential performance indication.

## V. DMM PHASE RESPONSE

Phase response of a single DMM is usually not of interest and is also never specified by the DMM manufacturer. However, numerous applications for measuring electrical power [18] make direct use of phase measurement using two sampling DMMs. To enable phase measurement, two DMM should be synchronised, either by a common trigger signal or operating in a master-slave fashion. To remove residual phase measurement errors due to various time delays of such setup, a known phase should be measured to provide for a reference point. An ideal 0 rad phase reference is a single sine wave signal at a given frequency, which is split to both DMM inputs using equal length cables. By interchanging the cables between two DMMs and comparing time delay results, the cable and DMM mismatch can be minimised.

While 3458A DMM has only an external trigger input to facilitate synchronisation, 8588A DMM adds a 1 MHz or 10 MHz external clock input, which greatly simplifies synchronous measurements using one or more 8588A. Unfortunately, it does not have any clock output.

To fully evaluate phase performance of the samplers, one would need to have an ideal phase source, which of course is not available. Instead, an arbitrary waveform generator Keysight 33622A and a custom made ČMI SWG03 high stability DDS source were used. Their performance directly influences results presented so the results should be viewed as a superposition of source and sampler results. A few different configurations were used in measurement with an attempt to discriminate which instrument is affecting a non-ideal result, with some success.

There are different phase characteristics that can be attributed to a pair of DMMs sampling a two channel signal. One is a phase linearity over the  $2\pi$  phase angle at single frequency and all sampling parameters (like sampling time, aperture time, range, signal level) being fixed. The other

Table IV  
SETTING FOR MASTER-SLAVE PHASE MEASUREMENTS AND RESULTS FOR  
ZERO PHASE MEASUREMENT. 3458A DMM AS MASTER AND 8588A AS  
SLAVE WERE USED.

$f$	$t_a$	$t_s$	$\Delta t_0$	$\Delta\phi_0$	$\Delta\phi_{dev}$
52 Hz	195 $\mu$ s	220 $\mu$ s	1.647 $\mu$ s	0.22 $\mu$ rad	0.70 $\mu$ rad
1 kHz	1.4 $\mu$ s	10 $\mu$ s	1.668 $\mu$ s	2.4 $\mu$ rad	1.5 $\mu$ rad
19 kHz	1.4 $\mu$ s	10 $\mu$ s	1.649 $\mu$ s	293 $\mu$ rad	6.8 $\mu$ rad

is a phase offset due to a trigger timing misalignment and different input circuitry phase delays, again at these same sampling parameters. Finally, these two characteristics can be measured at different frequencies to obtain their frequency dependent response. The phase results presented here were not performed thoroughly to give a full picture for either of them as the equipment used was not available for all those measurements. However, I hope they provide a sneak peek into what is possible to achieve in terms of phase accuracy over a reasonably large frequency bandwidth.

For all phase results presented in this paper, 7 V signals were used on 10 V DMM's range.

#### A. Master-Slave synchronisation

ČMI SWG03 source was used for these measurements. The settings given in Table IV were used. The 3458A DMM was operating in a DCV mode, while 8588A DMM was operating in DCV mode only for 52 Hz signal frequency. 100 000 samples were taken for each phase measurement and 10 repetitions were performed at each phase setting. As the 3458A DMM was used as a master DMM for final results, the synchronisation was not possible and thus a PSFE algorithm [25] was used to retrieve phase results.

The following steps were performed:

- 1) A single source channel was connected in parallel to both DMMs using a T-piece and a same length cables. By measuring residual phase,  $\Delta t_0$  was determined at each frequency, indicating a cumulative time delay between master and slave DMM.
- 2) Source phase was programmed to  $0^\circ$ , both channels were connected to corresponding DMMs and the phase was measured again, taking into account a residual phase obtained in the previous step ( $\Delta t_0$ ). This resulted in a zero phase difference  $\Delta\phi_0$ .
- 3) Source phase between two channels was increased in steps of  $30^\circ$  to obtain phase linearity results within  $\pm\Delta\phi_{dev}$  as shown on figures 21, 22 and 23. These results are normalised to start from 0 rad. Vertical bars represent standard deviations obtained from ten repetitions at each frequency and phase setting.

A question will certainly appear as to why the 3458A DMM was used as a master, rendering the clock synchronisation impossible. This decision was made based on preliminary experiments, which showed that this configuration is far superior form using 8588A DMM as a master. This is demonstrated on Figure 24, where 8588A served as a master with all other

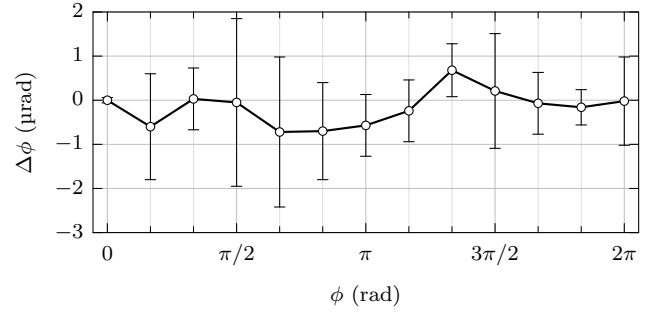


Figure 21. Phase response at 52 Hz for 3458A DMM (master) and 8588A DMM (slave) configuration.

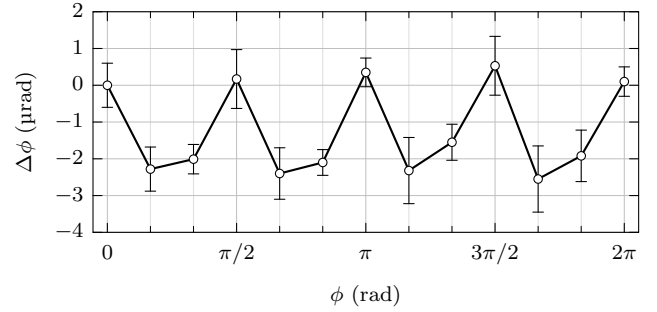


Figure 22. Phase response at 1 kHz for 3458A DMM (master) and 8588A DMM (slave) configuration on 10 V range.

settings remaining exactly the same as for the results shown on Figure 22, in this case for  $f = 1$  kHz. Additionally, the same difference was observed at other signal frequencies.

No further research was done to find the reason for such behaviour and therefore no explanation can be provided at this point. Unfortunately, no phase measurements were performed with ČMI SWG03 source and two 8588A as when an operational source arrived, one 8588A DMM needed to be returned.

Another example is provided here for additional info only. The ČMI SWG03 source software platform offers a DAC alignment mode. This alignment secures a generation of an identical signal even when changing its phase. This is achieved by programming DACs with exactly the same words, regardless of the phase setting. The price paid is that the phase

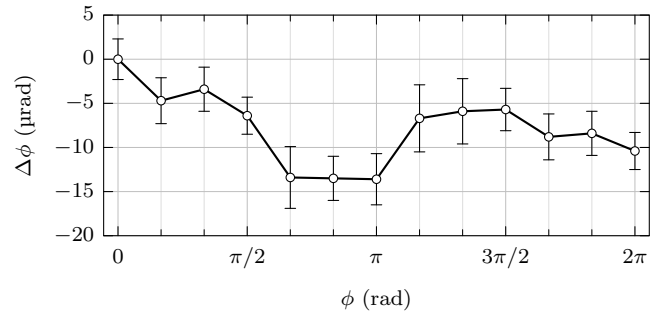


Figure 23. Phase response at 19 kHz for 3458A DMM (master) and 8588A DMM (slave) configuration on 10 V range.

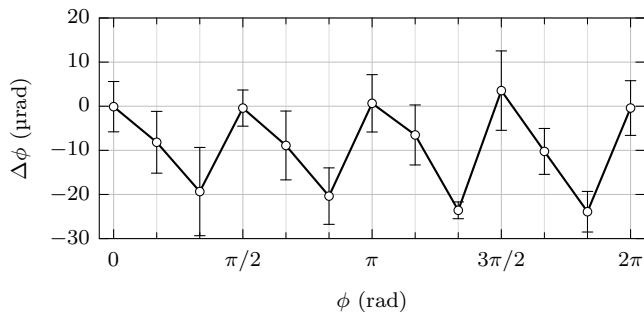


Figure 24. Phase response at 1 kHz for 8588A DMM (master) and 3458A DMM (slave) configuration on 10 V range.

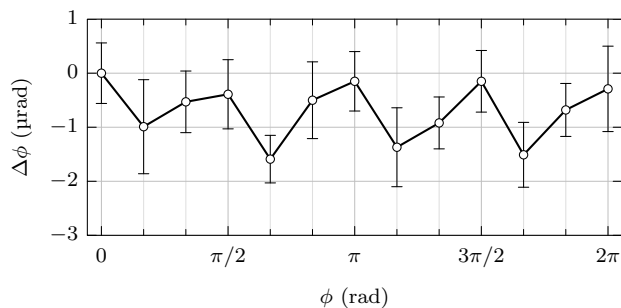


Figure 25. Phase response at 1 kHz for 3458A DMM (master) and 8588A DMM (slave) configuration on 10 V range. The source had a special function DAC aligned being enabled.

setting resolution is reduced, but the actual phase setting is always reported and could be used as a reference. The results from this experiment are presented on Figure 25. Comparing this with the results on Figure 24, we can observe slightly lower standard deviations and slightly better measured phase linearity. There is also a pattern seen on these results, repeating on every  $\pi/2$  rad phase change, that also appears on Figures 22 and 24. This could be related to an effect of high frequency glitches coming from source DAC's steps, noting that DAC steps and glitches are hardly filtered out completely.

### B. Common clock synchronisation

For synchronous measurements, two 8588A DMMs were used with a common 10 MHz clock supplied from Keysight 33622A arbitrary waveform synthesizer. They were still configured in a master-slave fashion using Trig Out and Trig In connectors. Both DMMs were configured to operate in Digitizing mode, using a SAR DAC. 20000 samples were taken for each phase measurement and 10 repetitions were performed at each phase setting. The setting given in Table V were used.

As the sampling was synchronous, all results were obtained using FFT. The same procedure was used as for the master-slave configuration. Results are presented on figures 26, 27, 28 and 29.

While these results are quite promising, they do not show whether source or DMMs are responsible for non-linearity at 1 kHz and 11 kHz, where the standard deviations are much smaller than this non-linearity.

Table V  
SETTING FOR CLOCK SYNCHRONISED MASTER-SLAVE PHASE MEASUREMENTS AND RESULTS FOR ZERO PHASE MEASUREMENT. TWO 8588A DMM WERE USED.

$f$	$t_a$	$t_s$	$\Delta t_0$	$\Delta\phi_0$	$\Delta\phi_{dev}$
1.107 kHz	48 $\mu$ s	50 $\mu$ s	104.68 ns	-42.7 $\mu$ rad	29 $\mu$ rad
11.075 kHz	18 $\mu$ s	20 $\mu$ s	104.73 ns	-6.7 $\mu$ rad	36 $\mu$ rad
110.75 kHz	0.6 $\mu$ s	1 $\mu$ s	104.80 ns	49.7 $\mu$ rad	15 $\mu$ rad
998.7 kHz	0.1 $\mu$ s	0.4 $\mu$ s	104.82 ns	1375 $\mu$ rad	38 $\mu$ rad

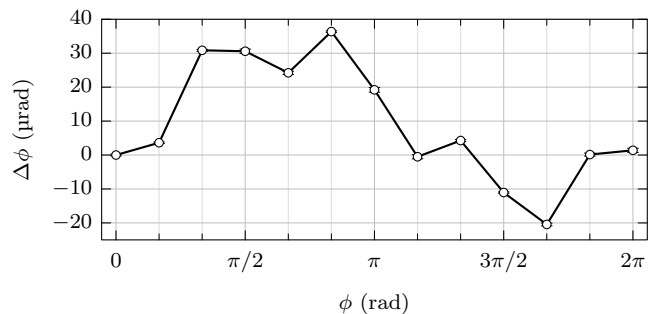


Figure 26. Phase response at 1 kHz for two 8588A DMM using a common external 10 MHz clock and internal TIMER for sampling instants.

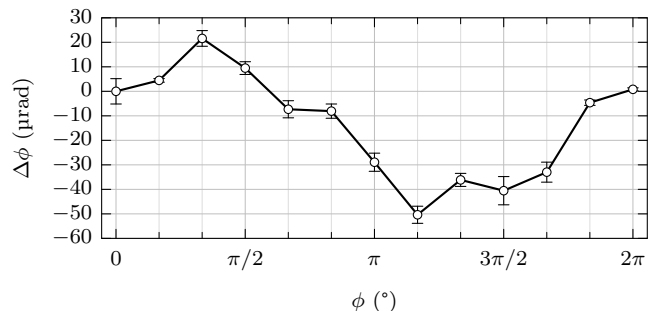


Figure 27. Phase response at 11 kHz for two 8588A DMM using a common external 10 MHz clock and internal TIMER for sampling instants.

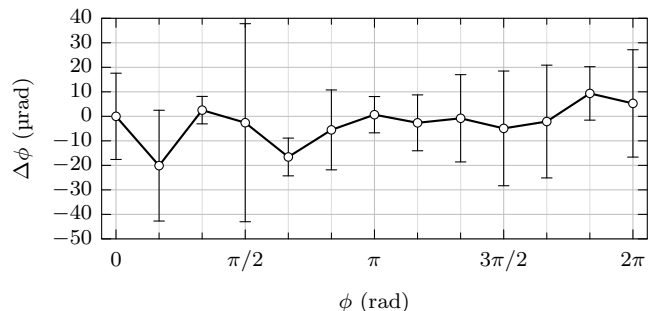


Figure 28. Phase response at 110 kHz for two 8588A DMM using a common external 10 MHz clock and internal TIMER for sampling instants.

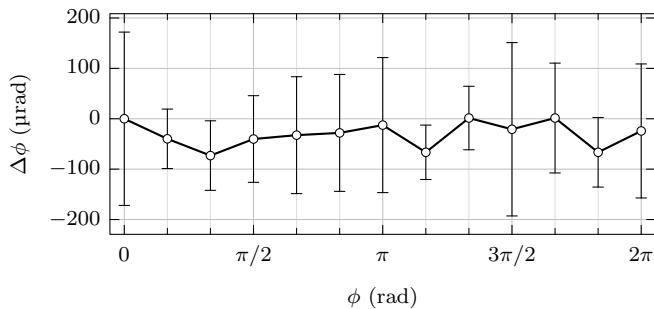


Figure 29. Phase response at 1 MHz for two 8588A DMM using a common external 10 MHz clock and internal TIMER for sampling instants. Measurements performed on 10 V range.

## VI. DISCUSSION

The 8588A DMM is a first serious challenge for 3458A DMM dominance in state of the art sampling accuracy at low frequencies. It sports a huge internal memory, all modern interface options and a clock input for timing synchronisation. Its functionality limits a direct use of integrating ADC for relatively slow sampling ( $f_s \leq 4.7619$  kHz). While its CB path design incorporates a zero drift amplifier technology which effectively pushes  $1/f$  noise corner to extremely low frequencies, the price paid is a much elevated white noise floor as well as quite inferior jitter performance, both as compared to 3458A DMM. This makes the 8588A DMM extremely suitable for measuring DC (and extremely low frequencies) signals. However, the available frequency band in this mode is limited and combined with elevated white noise, timing jitter and harmonic distortions, the 8588A overall sampling performance is inferior already for sampling 50 Hz frequency signals.

For sampling faster signals, the 8588A DMM relies on averaging 18 bit SAR ADC technology for sampling frequencies up to 5 MHz. The performance of this digitising mode looks excellent, but it no longer holds the same DC accuracy,  $1/f$  noise corner and stability demonstrated by CB path. Additionally, it is not clear if this mode surpasses the commercial SAR ADC technology available and how it will cope with a very rapid developments in this field. It is unlikely it would achieve and maintain the same dominance as 3458A IADC did over the last 30 years.

## VII. FURTHER WORK

It would be interesting to compare the actual DC linearity of 3458A and 8588A DMMs with a DC Josephson source. Additionally, phase performance should be measured more accurately, as it is quite possible that the results presented here were influenced more by a source than by a DMMs. Certainty, further investigations of this new DMM will reveal its performance in specific areas and applications.

## ACKNOWLEDGMENT

The author would like to thank Fluke Corporation and Micom to lend two 8588A DMMs for a substantial amount of time, Matjaž Lindič from SIQ for lending Keysight 3458A

and 33622A instruments and Jan Kučera from ČMI for lending their SWG03 source. A special thanks goes to Boštjan Voljč, being always ready to help with virtually everything I needed.

## REFERENCES

- [1] R. L. Swerlein, *A 10 ppm accurate digital AC Measurement algorithm*, Agilent Technologies, 1991.
- [2] M. E. Cage, D. Yu, B. M. Jeckelmann, R. L. Steiner, and R. V. Duncan, "Investigating the Use of Multimeters to Measure Quantized Hall Resistance Standards," *IEEE Trans. Instrum. Meas.*, vol. 40, no. 2, pp. 262–266, 1991.
- [3] S. Svensson, "A Precision Wattmeter for Non-sinusoidal Conditions," Chalmers University of Technology, Gothenburg, Sweden, Technical Report No. 223L, 1996.
- [4] G. Ramm, H. Moser, and A. Braun, "A New Scheme for Generating and Measuring Active, Reactive, and Apparent Power at Power Frequencies with Uncertainties of  $2.5 \times 10^{-6}$ ," *IEEE Trans. Instrum. Meas.*, vol. 48, pp. 422–426, 1999.
- [5] W. G. K. Ihlenfeld, "Maintenance and Traceability of AC Voltages by Synchronous Digital Synthesis and Sampling," PTB-Bericht PTB-E-75, Braunschweig, Tech. Rep., 2001.
- [6] E. Mohns, G. Ramm, W. G. K. Ihlenfeld, L. Palafox, and H. Moser, "The PTB Primary Standard for Electrical AC Power," *Journal of Metrology Society of India*, vol. 24, no. 1, pp. 15–19, 2009.
- [7] R. Iuzzolino and W. G. K. Ihlenfeld, "High-Accuracy Methods and Measurement Procedures for Power Quality Parameters Using the Digital Synchronous Sampling Technique," *IEEE Trans. Instrum. Meas.*, vol. 56, no. 2, pp. 426–430, April 2007.
- [8] P. Espel, A. Poletaeff, and A. Bounouh, "Characterization of analogue-to-digital converters of a commercial digital voltmeter in the 20 Hz to 400 Hz frequency range," *Metrologia*, vol. 46, pp. 578–584, 2009.
- [9] P. Horowitz and W. Hill, *The art of electronics*, 3rd ed. Cambridge University Press, 2015.
- [10] J. Kučera, J. Kováč, L. Palafox, R. Behr, and V. Vojáčková, "Characterization of a precision modular sinewave generator," *Meas. Sci. Technol.*, vol. 31, pp. 1–9, 2020.
- [11] *Keysight Trueform Series Waveform Generator, Operating and Service Guide*, Keysight, Nov. 2020.
- [12] *3457A Multimeter Operating Manual*, Hewlett-Packard, May 1986.
- [13] Hewlett-Packard, *Hewlett-Packard Journal*, April 1987.
- [14] Fluke Calibration, "A/D Converter Technology," Fluke Calibration, Tech. Rep., 2019.
- [15] *8588A/8558A Reference Multimeter and 8<sup>1/2</sup> Digit Multimeter Operators Manual*, Fluke Calibration, Feb. 2019.
- [16] *8588A Reference Multimeter Product Specifications, Rev. B, 4/19*, Fluke Calibration, March 2019.
- [17] W. C. Goecke, "An 8<sup>1/2</sup>-Digit Integrating Analog-to-Digital Converter with 16-Bit, 100,000-Sample-per-Second Performance," *Hewlett-Packard Journal*, vol. 40, pp. 8–15, 1989.

- [18] P. Horowitz and W. Hill, *Sampling with 3458A, Understanding, Programming, Sampling and Signal Processing*, 1st ed. Left Right d.o.o., 2018.
- [19] R. Lapuh, B. Voljč, and M. Lindič, “Keysight 3458A Noise Performance,” in *Conference on Precision Electromagnetic Measurements (CPEM)*, 2016, pp. 1–2.
- [20] W. Heinzl, A. Rüdiger, and R. Schilling, “Spectrum and spectral density estimation by the Discrete Fourier Transform (DFT), including a comprehensive list of window functions and some new flat-top windows.” Max-Planck-Institut für Gravitationsphysik, Tech. Rep., 2002, also available as <http://pubman.mpg.de/pubman/item/escidoc:152164:1/component/escidoc:152163/395068.pdf>.
- [21] R. Lapuh, B. Voljč, and M. Lindič, “Evaluation of Agilent 3458A Time Jitter Performance,” *IEEE Trans. Instrum. Meas.*, vol. 64, no. 6, pp. 1331–1335, June 2015.
- [22] R. Lapuh and R. Lapuh, “Keysight 3458A Frequency Response Model Identification,” in *Conference on Precision Electromagnetic Measurements (CPEM)*, 2018, pp. 1–2.
- [23] S. W. Smith, *The Scientist & Engineer's Guide to Digital Signal Processing*. California Technical Pub, 1997, also available at <http://www.dspguide.com/>.
- [24] G. B. Gubler, “Reconstruction of bandlimited signal using samples obtained from integration digital voltmeters,” in *Conference on Precision Electromagnetic Measurements (CPEM)*, 2010, pp. 257–258.
- [25] R. Lapuh, “Estimating the Fundamental Component of Harmonically Distorted Signals From Noncoherently Sampled Data,” *IEEE Trans. Instrum. Meas.*, vol. 64, no. 6, pp. 1419–1424, June 2015.
- [26] J. Schoukens, R. Pintelon, and G. Vandersteen, “A sinewave fitting procedure for characterizing data acquisition channels in the presence of time base distortion and time jitter,” *IEEE Trans. Instrum. Meas.*, vol. 46, no. 4, pp. 1005–1010, 1997.